JACS
JOURNAL OF THE AMERICAN CHEMICAL SOCIETY
Article
pubs.acs.org/JACS

NMR Study on the B–Z Junction Formation of DNA Duplexes Induced by Z-DNA Binding Domain of Human ADAR1

Yeon-Mi Lee,[†,#] Hee-Eun Kim,[†,#] Chin-Ju Park,[‡] Ae-Ree Lee,[†] Hee-Chul Ahn,[§] Sung Jae Cho,[∥] Kwang-Ho Choi,[†] Byong-Seok Choi,*[,∥] and Joon-Hwa Lee*[,†]

[†]Department of Chemistry and RINS, Gyeongsang National University, Jinju, Gyeongnam 660-701, Republic of Korea
[‡]School of General Studies, Gwangju Institute of Science and Technology, Gwangju 500-712, Republic of Korea
[§]College of Pharmacy, Dongguk University, Goyang, Gyeonggi 410-774, Republic of Korea
[∥]Department of Chemistry, Korea Advanced Institute of Science and Technology, Daejeon 305-701, Republic of Korea.

Supporting Information

ABSTRACT: Z-DNA is produced in a long genomic DNA by Z-DNA binding proteins, through formation of two B–Z junctions with the extrusion of one base pair from each junction. To answer the question of how Z-DNA binding proteins induce B–Z transitions in CG-rich segments while maintaining the B-conformation of surrounding segments, we investigated the kinetics and thermodynamics of base-pair openings of a 13-bp DNA in complex with the Z-DNA binding protein, $Z\alpha_{ADAR1}$. We also studied perturbations in the backbone of $Z\alpha_{ADAR1}$ upon binding to DNA. Our study demonstrates the initial contact conformation as an intermediate structure during B–Z junction formation induced by $Z\alpha_{ADAR1}$, in which the $Z\alpha_{ADAR1}$ protein displays unique backbone conformational changes, but the 13-bp DNA duplex maintains the B-form helix. We also found the unique structural features of the 13-bp DNA duplex in the initial contact conformation: (i) instability of the AT-rich region II and (ii) longer lifetime for the opening state of the CG-rich region I. Our findings suggest a three-step mechanism of B–Z junction formation: (i) $Z\alpha_{ADAR1}$ specifically interacts with a CG-rich DNA segment maintaining B-form helix via a unique conformation; (ii) the neighboring AT-rich region becomes very unstable, and the CG-rich DNA segment is easily converted to Z-DNA; and (iii) the AT-rich regions are base-paired again, and the B–Z junction structure is formed.

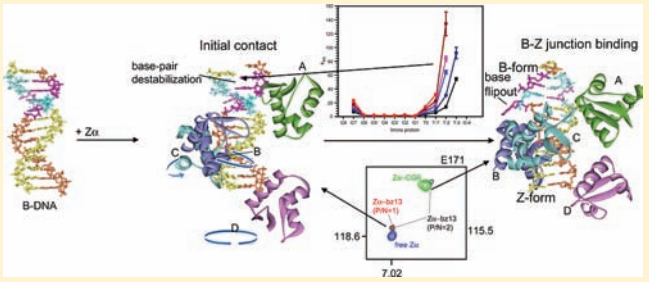

INTRODUCTION

Left-handed Z-DNA is a higher energy conformation than B-DNA and is stabilized by negative supercoiling generated in vivo.[1,2] Z-DNA forms in polymers of alternating $d(CG)_n$ under high-salt conditions,[3] and its structure was first reported in an X-ray crystallographic study in 1979.[4] Z-DNA is also stabilized by interaction with Z-DNA-specific binding proteins with nanomolar binding constants.[5−9] One such protein, double-stranded RNA deaminase I (ADAR1), has two left-handed Z-DNA binding domains, Zα and Zβ, at its N-terminus.[10] The crystal structure of the Zα domain of human ADAR1 ($Z\alpha_{ADAR1}$) complexed to Z-DNA revealed that one monomeric Zα domain binds to one strand of double-stranded Z-DNA, while a second monomer binds to the opposite strand, yielding two-fold symmetry with respect to the DNA helical axis.[5] Z-DNA binding domains are also found in the poxvirus E3L protein, the human DNA-dependent activator of IFN-regulatory factor (DAI), and the fish PKZ protein kinase.[7,9,11] The overall structures of Zα domains of yatapoxvirus E3L and mouse DAI and their interactions with Z-DNA are very similar to those of $Z\alpha_{ADAR1}$.[6,8] Recent NMR studies of the $d(CGCGCG)_2$–$Z\alpha_{ADAR1}$ complex have suggested an active B–Z transition mechanism, in which the $Z\alpha_{ADAR1}$ protein first binds to B-DNA and then converts a 6-base-pair (6-bp) stretch to left-handed Z-DNA, a conformation that is then stabilized by the additional binding of a second $Z\alpha_{ADAR1}$ molecule.[12]

When Z-DNA is produced in a section of long genomic DNA by Z-DNA binding proteins, two B–Z junctions, which cause little structural disruption and preserve helix integrity, should be formed. An X-ray structural study of a 15-bp DNA duplex complexed with $Z\alpha_{ADAR1}$ showed that DNA helices are stabilized at one end in the Z-conformation by $Z\alpha_{ADAR1}$ proteins, while the other end remains B-DNA.[13] This study also found that bases between B- and Z-DNA are almost continuously stacked with the breaking of only one base pair at the junction and extrusion of each base.[13] Even though this structural study proved the existence of B–Z junction in a DNA helix, the question of how Z-DNA binding proteins selectively induce a B–Z transition in CG-rich DNA segment while maintaining the B-conformation in other segments and the integrity of overall helix remains. In order to answer this

Received: December 12, 2011
Published: February 17, 2012

   dx.doi.org/10.1021/ja211581b | J. Am. Chem. Soc. 2012, 134, 5276–5283

question, we have conducted an NMR study on complexes between $Z\alpha_{ADAR1}$ and a 13-bp DNA duplex (referred to as bzDNA13, Figure 1a), which exist in multiple protein-to-DNA

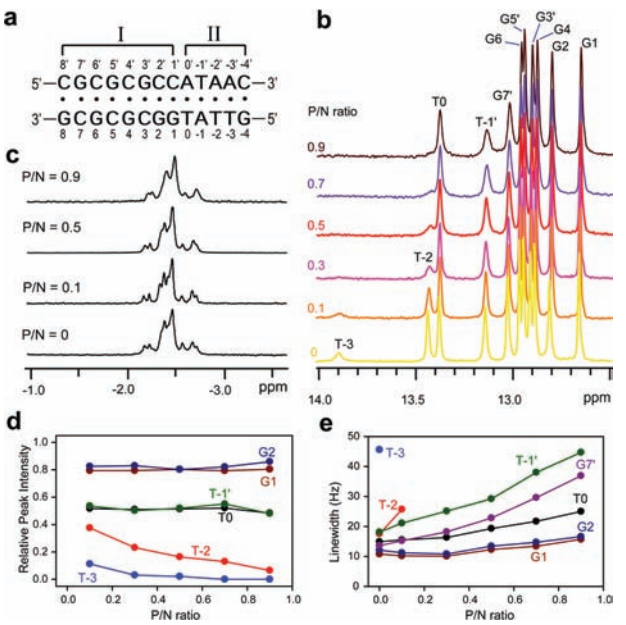

Figure 1. (a) Sequence context of the bzDNA13 DNA duplex studied here. (b) 1D imino proton and (c) ^{31}P NMR spectra of free bzDNA13 and bzDNA13–$Z\alpha_{ADAR1}$ complexes at various P/N ratios. The P/N ratios are shown to the left of each spectrum. (d) Relative peak intensities and (e) line widths of imino proton resonances in the bzDNA13–$Z\alpha_{ADAR1}$ complexes as a function of the P/N ratio.

(P/N) molar ratios. The DNA sequence of bzDNA13 is basically the same as that of the previous X-ray study,[13] but the two structurally expendable base pairs in region II are removed to avoid resonance overlap. The hydrogen exchange rate constants (k_{ex}) for the imino protons of the bzDNA13 in the complexes were determined as a function of the P/N ratios by NMR spectroscopy. We investigated the kinetics and thermodynamics of base-pair openings of the bzDNA13 in the complexes at various P/N ratios using TRIS as a base catalyst. The chemical shift perturbations in the amide backbone of $Z\alpha_{ADAR1}$ were also studied as a function of the P/N ratios. This study reveals key features of the intermediate of structures of the $Z\alpha_{ADAR1}$–bzDNA13 complex and provides the information about the molecular mechanism of B–Z junction formation.

EXPERIMENTAL SECTIONS

Sample Preparation. The DNA oligomers, d(CGCGCGCCATAAC) and d(GTTATGGCGCGCG), were purchased from IDT Inc. The oligomers were purified by reverse-phase HPLC and desalted using a Sephadex G-25 gel filtration column. The DNA duplex was prepared by dissolving two DNA strands at a 1:1 stoichiometric ratio in a 90% H_2O/10% D_2O NMR buffer containing 10 mM sodium phosphate (pH 8.0) and 100 mM NaCl. To produce ^{15}N-labeled $Z\alpha_{ADAR1}$, BL21(DE3) bacteria were grown in M9 medium containing 1 g/L $^{15}NH_4Cl$. Expression and purification of ^{15}N-labeled $Z\alpha_{ADAR1}$ have been described in a previous report.[13] The protein concentration was measured spectroscopically using an extinction coefficient of 6970 $M^{-1}cm^{-1}$ at 280 nm.

NMR Experiments. All ^{1}H and ^{15}N NMR experiments were performed on a Varian 900 MHz (KIST, Seoul) or Agilent DD2 700 MHz NMR spectrometer (GNU, Jinju) equipped with a cryoprobe. The ^{31}P NMR experiments were performed on a Varian 500 MHz NMR spectrometer (Agilent Technologies Korea, Seoul). All ^{1}H, ^{15}N, and ^{31}P NMR spectra were obtained using complex samples which were prepared by the addition of ^{15}N-labeled $Z\alpha_{ADAR1}$ to 0.2 mM DNA samples in NMR buffer at the indicated P/N ratio. One-dimensional (1D) NMR data were processed with either the program VNMR J (Agilent, Santa Clara) or FELIX2004 (Accelrys, San Diego), whereas 2D data were processed with the program NMRPipe[14] and analyzed with the program Sparky.[15] External 2-2-dimethyl-2-silapentane-5-sulfonate was used for the ^{1}H and ^{15}N references, and sodium phosphate was used as the ^{31}P reference.

The average chemical shift differences of the amide proton and nitrogen resonances between the free $Z\alpha_{ADAR1}$ and $Z\alpha_{ADAR1}$ in complex with CG6 or bzDNA13 were calculated by using eq 1:

$$\Delta\delta_{avg} = \sqrt{(\Delta\delta_H)^2 + (\Delta\delta_N/5.88)^2} \quad (1)$$

where $\Delta\delta_H$ and $\Delta\delta_N$ are the chemical shift differences of the amide proton and nitrogen resonances, respectively.

Hydrogen Exchange Rate Measurement. The apparent longitudinal relaxation rate constants ($R_{1a} = 1/T_{1a}$) of the imino protons of free bzDNA13 and the bzDNA13–$Z\alpha_{ADAR1}$ complexes at various P/N ratios were determined by semiselective inversion recovery 1D NMR experiments. The apparent relaxation rate constant of water (R_{1w}) was determined by a selective inversion recovery experiment, using a DANTE sequence for selective water inversion.[16] R_{1a} and R_{1w} were determined by curve fitting of the inversion recovery data to the appropriate single-exponential function. The hydrogen exchange rate constants (k_{ex}) of the imino protons were measured by a water magnetization transfer experiment. The intensities of each imino proton were measured with 20 different delay times. The k_{ex} values for the imino protons were determined by fitting the data to eq 2:

$$\frac{I_0 - I(t)}{I_0} = 2\frac{k_{ex}}{(R_{1w} - R_{1a})}(e^{-R_{1a}t} - e^{-R_{1w}t}) \quad (2)$$

where I_0 and $I(t)$ are the peak intensities of the imino proton in the water magnetization transfer experiments at times zero and t, respectively, and R_{1a} and R_{1w} are the apparent longitudinal relaxation rate constants for the imino proton and water, respectively, measured in semiselective inversion recovery 1D NMR experiments.[16,17]

The formalism of TRIS-catalyzed proton exchange has been previously described in detail in the previous studies[16,18,19] and is briefly presented here. The exchange time for the base-paired imino proton, τ_{ex} (inverse of k_{ex}), is represented by:

$$\tau_{ex} = \tau_0 + \frac{1}{\alpha K_{op} k_i}\frac{1}{[TRIS]} \quad (3)$$

where τ_0 is the base-pair lifetime (the inverse of opening rate constant, or $1/k_{op}$), k_i is the rate constant for imino proton transfer, and αK_{op} (= $\alpha k_{op}/k_{cl}$) is the apparent equilibrium constant for base-pair opening.

RESULTS

Titration of $Z\alpha_{ADAR1}$ into bzDNA13. 2D nuclear Overhauser enhancement spectroscopy (NOESY) spectra were used to assign the imino proton resonances of the bzDNA13 DNA duplex. Figure 1b shows the 1D imino proton spectra of the bzDNA13–$Z\alpha_{ADAR1}$ complexes at various P/N ratios. As the P/N ratio is increased, the peak intensities for the T–2 and T–3 protons significantly decreased until they completely disappeared at P/N ratio = 0.9 (Figure 1b). These results demonstrate that the T–2·A–2′ and T–3·A–3′ base pairs of bzDNA13 are significantly destabilized upon binding to $Z\alpha_{ADAR1}$ protein. However, $Z\alpha_{ADAR1}$ binding did not affect the peak intensities for other resonances when the P/N ratio was <1.0 (Figure 1d). Interestingly, the T–1′ resonance became clearly broadened as the P/N ratio is increased, even though its intensity was not affected (Figure 1b,e). The $Z\alpha_{ADAR1}$ also

dx.doi.org/10.1021/ja211581b | J. Am. Chem. Soc. 2012, 134, 5276–5283

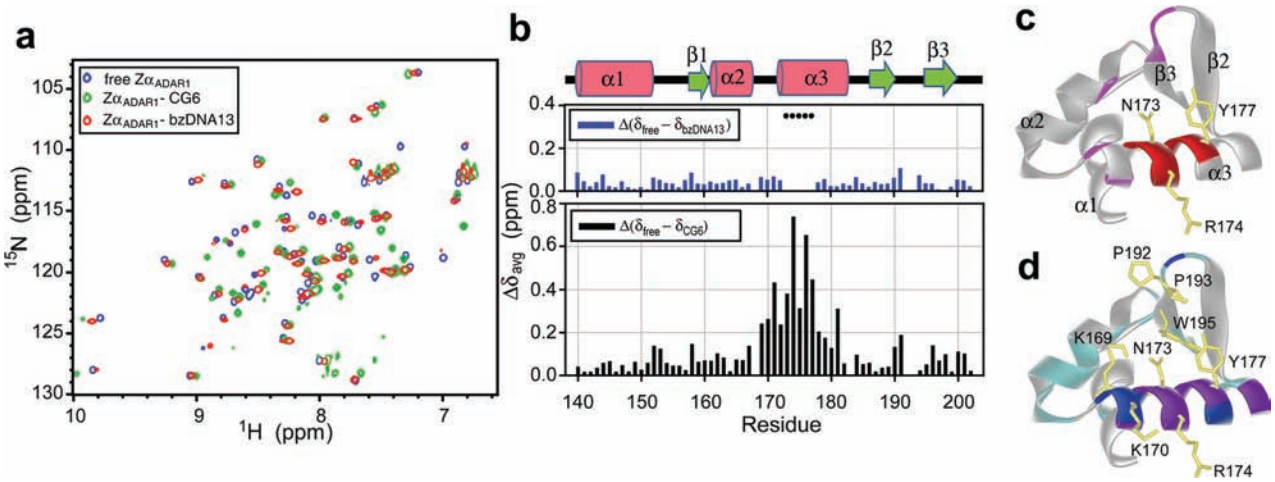

Figure 2. (a) Superimposition of $^{1}H/^{15}N$-HSQC spectra of free $Z\alpha_{ADAR1}$ (blue), $Z\alpha_{ADAR1}$−CG6 complex (P/N = 2, green) and $Z\alpha_{ADAR1}$−bzDNA13 complex (P/N = 1, red) at 35 °C. (b) Blue and black bars are weighted average $^{1}H/^{15}N$ chemical shift changes ($\Delta\delta_{avg}$) of $Z\alpha_{ADAR1}$ upon binding to bzDNA13 (P/N = 1, blue) and CG6 (P/N = 2, black). Residues whose cross-peaks disappear in the $^{1}H/^{15}N$-HSQC spectrum of the $Z\alpha_{ADAR1}$−bzDNA13 complex are indicated with black circles. When amide resonances of the residues were not observed in the spectrum of free $Z\alpha_{ADAR1}$ at 35 °C, chemical shift values at 25 °C were used in the calculation. (c) Mapping of the $Z\alpha_{ADAR1}$ residues with chemical shift perturbations caused by binding of bzDNA13 (PDB ID = 1QBJ). Residues with chemical shift changes of 0.07−0.15 ppm are indicated in pink. Residues whose amide resonances disappeared upon binding to bzDNA13 are indicated in red. (d) Chemical shift perturbation mapping of the $Z\alpha_{ADAR1}$ bound to CG6 (PDB ID = 1QBJ). Color used to illustrate $^{1}H/^{15}N$ chemical shift changes upon CG6 binding are: purple, > 0.3 ppm; blue, 0.15−0.3 ppm; and cyan, 0.07−0.15 ppm.

caused a slight line broadening for other imino proton resonances (Figure 1e), without including any chemical shift changes. ^{31}P chemical shifts are a sensitive probe of unusual backbone conformations of oligonucleotides and are especially valuable for studying B−Z transitions induced by the Z-DNA binding proteins. Surprisingly, all ^{31}P spectra of the bzDNA13−$Z\alpha_{ADAR1}$ complex showed the same chemical shift dispersion as that of free bzDNA13 (Figure 1c). This indicates that, when the P/N ratio is <1, the bzDNA13 duplex is not yet converted to Z-DNA but maintains a B-form helix, even though the imino proton resonances are affected by the DNA−protein interaction.

When the P/N ratio is >1, the 1D imino proton spectra significantly change until the P/N ratio reaches 4.5, and the line-broadening effect induced by the $Z\alpha_{ADAR1}$ is observed more clearly (Figure S8a, Supporting Information). Interestingly, the ^{31}P spectrum of the bzDNA13−$Z\alpha_{ADAR1}$ complex at P/N = 4.5 dispersed over 3 ppm, whereas the resonances for free bzDNA13 appeared in the range of −2.5 to −2.9 ppm (Figure S8b, Supporting Information), like $d(CGCGCG)_2$ (referred to as CG6) in a previous study.[12] These results indicated that the bzDNA13 duplex converted to the B−Z junction structure through binding with four molecules of $Z\alpha_{ADAR1}$, which is consistent with the crystal structure previously reported.[13] The severe line broadening in the imino proton and ^{31}P spectra of the bzDNA13−$Z\alpha_{ADAR1}$ complex at P/N = 4.5 resulted from the very large molecular size compared to free bzDNA13 (38 versus 8 kDa).

Chemical Shift Perturbation of $Z\alpha_{ADAR1}$ upon Binding to bzDNA13 at P/N ≤ 1. The NMR fingerprint created by the amide backbone resonances of the $Z\alpha_{ADAR1}$−CG6 complex (P/N = 2)[12] was used as a structural probe for the $Z\alpha_{ADAR1}$−bzDNA13 complex. As shown in Figure 2a, the $^{1}H/^{15}N$-HSQC spectrum of the $Z\alpha_{ADAR1}$−bzDNA13 complex (P/N = 1) is completely different from that of the $Z\alpha_{ADAR1}$−CG6 complex (P/N = 2). In the $Z\alpha_{ADAR1}$−CG6 complex, all residues of the α3 helix undergo significant backbone chemical shift changes ($\Delta\delta_{avg}$ > 0.15 ppm) upon binding to the CG6 substrate (Figure 2b).[12] In addition, significant chemical shift changes were observed in the β1−α2 and β2−loop−β3 regions of the $Z\alpha_{ADAR1}$−CG6 complex (Figure 2b).[12] These significant chemical shift perturbations suggest direct interaction of the correspoding residues with the phosphate backbone of the CG6, as reported in the previous crystal structural study (Figure 2d).[5] In contrast, the residues of $Z\alpha_{ADAR1}$ underwent $\Delta\delta_{avg}$ < 0.15 ppm upon binding to the bzDNA13 duplex, when the P/N ratio =1. Surprisingly, in the $Z\alpha_{ADAR1}$−bzDNA13 complex (P/N = 1), the amide resonances for five residues (173−177) of the α3 helix disappeared altogether (Figure 2b), meaning they were in chemical exchange on an intermediate NMR time scale. The same patterns in the $^{1}H/^{15}N$-HSQC spectra were observed for the $Z\alpha_{ADAR1}$−bzDNA13 complexes when the P/N ratio ≤ 1 (data not shown). These $^{1}H/^{15}N$-HSQC spectra show that, while the $Z\alpha_{ADAR1}$ in complex with bzDNA13 at P/N ≤ 1 is different from free $Z\alpha_{ADAR1}$, it is also distinct from the $Z\alpha_{ADAR1}$ in complex with CG6 (Z-DNA).

Chemical Shift Perturbation of $Z\alpha_{ADAR1}$ upon Binding to bzDNA13 at P/N = 2. Figure 3 shows a superimposition of the $^{1}H/^{15}N$-HSQC resonances for some amide residues in free $Z\alpha_{ADAR1}$, $Z\alpha_{ADAR1}$−CG6 (P/N = 2), and $Z\alpha_{ADAR1}$−bzDNA13 (P/N = 1 and 2). The residues which showed little chemical shift perturbation upon binding to CG6, such as G153 and T156, have similar positions in the $^{1}H/^{15}N$-HSQC spectra of the $Z\alpha_{ADAR1}$−bzDNA13 complexes at both P/N = 1 and 2 (Figure 3a). The E171 amide signal in the $Z\alpha_{ADAR1}$−bzDNA13 complex at P/N = 1 is located closer to that of free $Z\alpha_{ADAR1}$ rather than the $Z\alpha_{ADAR1}$−CG6 complex (Figure 3b). Surprisingly, when the P/N ratio = 2, the $Z\alpha_{ADAR1}$−bzDNA13 complex exhibits two E171 amide signals; one is close to the free form signal, and the other to that for the $Z\alpha_{ADAR1}$−CG6 complex (Figure 3b). Similar results were also observed in the amide signals for A180 and G190 and the resonance for the W195 side-chain (Figure 3d−f). The Y177 residue shows no amide signal in the $Z\alpha_{ADAR1}$−bzDNA13

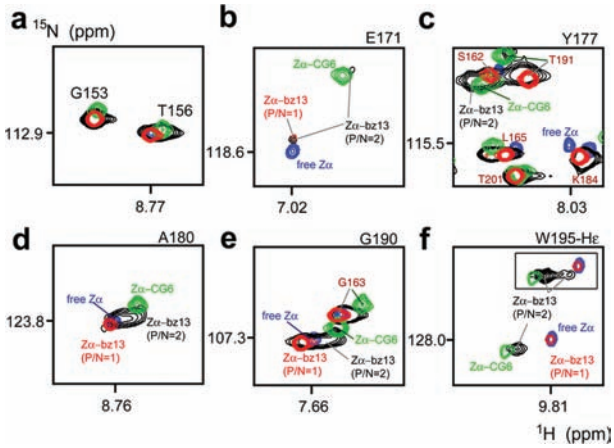

Figure 3. Comparison of the of ^{1}H/^{15}N-HSQC peaks of (a) G153 and T156, (b) E171, (c) Y177, (d) A180, and (e) G190 amide protons and (f) W195 side-chain of $Z\alpha_{ADAR1}$ in the free (blue) and complexes with CG6 at P/N = 2 (green) and bzDNA13 at P/N = 1 (red) and 2 (black) at 35 °C. The ^{1}H/^{15}N-HSQC spectra, in which the threshold of spectra for the only bzDNA13−$Z\alpha_{ADAR1}$ complex at P/N ratio = 2 is decreased, are shown in the inset box of (f). Residues colored brown indicate the amide signals which were not for Y177 in (c) or G190 in (e).

complex at P/N = 1 as described above, but, when the P/N ratio = 2, its amide resonance is observed near the corresponding signal of the ZαADAR1−CG6 complex (Figure 3c). Taken together, we can summarize that: (i) when the P/N ≤ 1, the ZαADAR1 exhibits a unique conformation (what we call the "initial contact" conformation) in which the protein interacts with bzDNA13 through mainly the α3 helix (Figure 2c) and (ii) when the P/N = 2, $Z\alpha_{ADAR1}$ exhibits properties of both the initial contact conformation and the Z-DNA-bound conformation, which is similar to the $Z\alpha_{ADAR1}$−CG6 complex (Figure 2d).

Exchange Rate Constants of Imino Protons of bzDNA13 Complexed with $Z\alpha_{ADAR1}$. In order to probe the interacting region of bzDNA13 with $Z\alpha_{ADAR1}$, the k_{ex} of the imino protons in free bzDNA13 and the bzDNA13−$Z\alpha_{ADAR1}$ complexes at various P/N ratios was determined at 35 °C by the water magnetization transfer method.[16,20] In free bzDNA13, rapidly exchanging imino protons, such as T−3 and T−2, show no peaks at a delay time of 75 ms, whereas the G1 imino resonance, which is the slowest exchanging imino proton, remains basically unchanged up to 100 ms (Figure 4a, left). Table S2, Supporting Information lists the k_{ex} values of the imino protons of the bzDNA13 duplex determined by curve fitting to eq 2. The T imino protons in the AT-rich region (region II) have k_{ex} from 3.0 to 54.4 s^{-1}, whereas, except for the terminal and C7·G7′ base pairs, the G imino protons in the CG-repeat region (region I) all have k_{ex} < 2.1 s^{-1}. These exchange data indicate that the base pairs in region I are much more stable than those in the region II at 35 °C.

In the bzDNA13−$Z\alpha_{ADAR1}$ complex at P/N = 0.9, the T−3 and T−2 imino proton resonances are disappeared at 35 °C (Figure 4a, right). In addition, in this complex, the T−1′ and T0 imino protons, whose resonances exhibit line broadening, show much larger differences in peak intensities as a function of delay time after water inversion compared to free bzDNA13 (Figure 4a). The k_{ex} values of the T−1′ (31.7 s^{-1}) and T0 (14.0 s^{-1}) imino protons in the bzDNA13−$Z\alpha_{ADAR1}$ complex at P/N = 0.9 are 6- and 5-fold larger than those of free bzDNA13, respectively (Figure 4b). Similarly, the G7′ imino proton in this complex has a k_{ex} value of 22.8 s^{-1}, which is 3-fold larger than that of free bzDNA13 (6.8 s^{-1}) (Figure 4b).

In order to clarify this observation, the k_{ex} of the imino protons in the bzDNA13−$Z\alpha_{ADAR1}$ complexes at various P/N ratios were determined at 35 °C and compared with those of free bzDNA13 (Figure 4b). In the bzDNA13−$Z\alpha_{ADAR1}$ complex at P/N = 0.1, the T−2 and T−3 imino protons have the k_{ex} values of 30.6 s^{-1} and 92.0 s^{-1}, respectively, which are 2-fold larger than those of free bzDNA13 (Table S2, Supporting Information). As the P/N ratio is increased, the k_{ex} value of the T−2 imino proton is increased up to 134.3 s^{-1} (Figure 4b and Table S2, Supporting Information). Because of

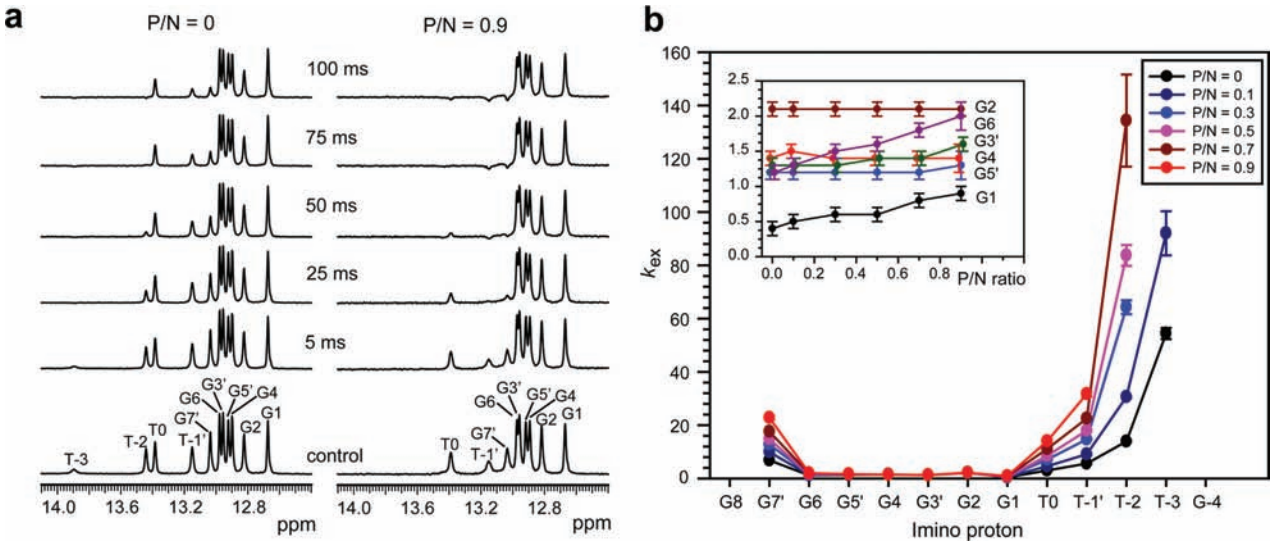

Figure 4. (a) 1D imino proton spectra of the water magnetization transfer experiments for free bzDNA13 (left) and the bzDNA13−$Z\alpha_{ADAR1}$ complex (P/N = 0.9, right) at 35 °C. The delay times after water inversion are shown between the two spectra. (b) The exchange rate constants of the imino protons of the bzDNA13−$Z\alpha_{ADAR1}$ complexes at various P/N ratios. The exchange rate constants of the central G imino protons of the bzDNA13−$Z\alpha_{ADAR1}$ complex as a function of the P/N ratio are shown in the inset box.

dx.doi.org/10.1021/ja211581b | J. Am. Chem. Soc. 2012, 134, 5276−5283

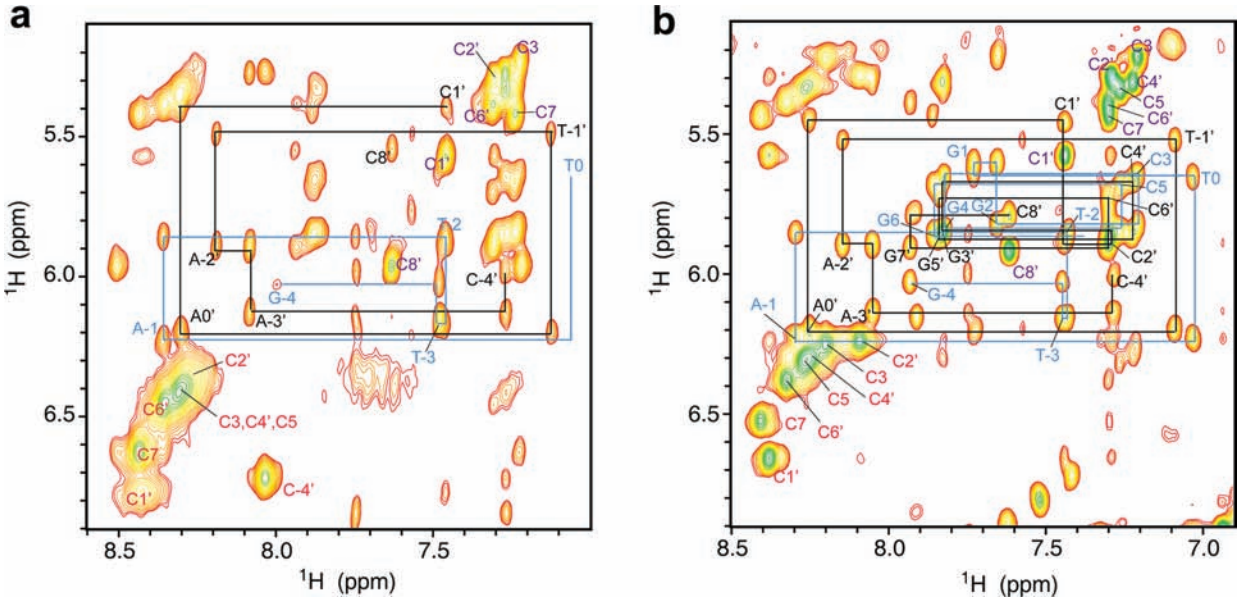

Figure 5. Watergate NOESY spectra of (a) free bzDNA13 (15 °C) and (b) the bzDNA13−Zα_{ADAR1} complex at P/N = 0.7 (35 °C). Solid lines indicate sequential NOE connectivities between base protons and their own and 5′ flanking sugar H1′ protons. Colors for residues used to distinguish the type of NOE crosspeaks: blue and black, H6/H8↔H1′; red, two amino protons; and purple, C−H5↔H6.

fast exchange, the T−2 imino proton resonance is extensively broadened and then not observed at P/N = 0.9 (Figure 1b). When the P/N ratio ≥ 0.3, the T−3 imino proton exchanged with solvent water too fast to be observed in 1D NMR spectra (see Figure 4a, right). Similarly, the G7′ and all T imino protons exchanged more rapidly with solvent water as the P/N ratio increased (Figure 4b). The k_{ex} values for the G1 and G6 imino protons increased slightly as the P/N ratio increased (Figure 4b). However, no enhancement of exchange was observed for other G imino protons in region I (Figure 4b). These results mean that the interaction of bzDNA13 with Zα_{ADAR1} significantly destabilizes four A·T base pairs in region II but had little effect on the k_{ex} values of the G·C base pairs in region I. Surprisingly, the sequential NOE connectivities between H6/H8 and H1′ protons for the AT-rich region II show no significant chemical shift differences between free bzDNA13 and the bzDNA13−Zα_{ADAR1} complex at P/N = 0.7 (Figure 5). The previous NMR study proved that the Zα_{ADAR1} proteins exhibit the sequence preference of d(CGCGCG)$_2$ ≫ d(CACGTG)$_2$ > d(CGTACG)$_2$ through multiple sequence discrimination steps during B−Z transition.[23] Thus, these indicate that, in the initial contact conformation, the Zα_{ADAR1} protein, while physically interacting with CG-rich region I, significantly destabilizes four A·T base pairs in AT-rich region II of bzDNA13.

Base Pair Opening Kinetics of bzDNA13−Zα_{ADAR1} Complexes at Various P/N ratios. Next, in order to understand the effect of Zα_{ADAR1} binding on the G·C base pairs in region I, the τ_{ex} (= $1/k_{ex}$) for each imino proton in the free bzDNA13 duplex, and the bzDNA13−Zα_{ADAR1} complexes (P/N = 0.3 or 0.9) were measured at 35 °C as a function of the inverse of TRIS concentration (Figure 6). From these data, the equilibrium constants for base-pair opening ($\alpha K_{op} = \alpha k_{op}/k_{cl}$) and the base-pair lifetimes ($\tau_0 = 1/k_{op}$) of the three duplexes were determined by curve fitting using eq 3 (Figure 6). In free bzDNA13, the six G·C base pairs in region I have $\alpha K_{op} \leq 5 \times 10^{-6}$ and τ_0 < 70 ms (Table 1). These data can be used to calculate an apparent lifetime for base-pair opening ($\alpha\tau_{open} = \alpha/k_{cl}$) of less than 100 ns (Table 1). The T0·A0′ (94×10^{-6}) and C7·G7′ (95×10^{-6}) base pairs have αK_{op} values larger than 90×10^{-6} (Table 1), indicating their relative instabilities compared to the six G·C base pairs in region I. In addition, the αK_{op} values for the other A·T base pairs in region II could not be determined because their resonances disappeared as the TRIS concentration increased.

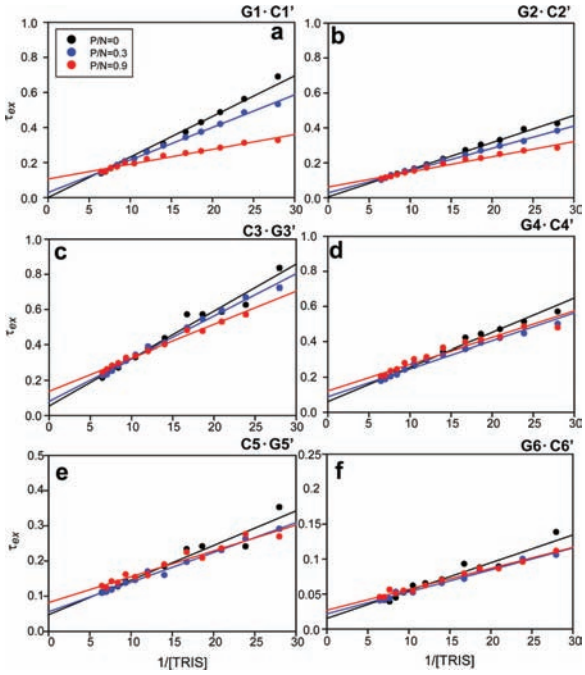

Figure 6. The hydrogen exchange times (τ_{ex}) of the (a) G1, (b) G2, (c) G3′, (d) G4, (e) G5′, and (f) G6 imino protons of the bzDNA13−Zα_{ADAR1} complexes at P/N ratio = 0 (black circle), 0.3 (blue circle), and 0.9 (red circle) as a function of the inverse of TRIS concentration at 35 °C. Solid lines indicate the best fit of these data using eq 3.

In Figure 6, the slope of the linear correlation between τ_{ex} of the imino proton and 1/[TRIS] is $1/(k_i\alpha K_{op})$ and the *y*-

dx.doi.org/10.1021/ja211581b | J. Am. Chem. Soc. 2012, 134, 5276−5283

Table 1. The αK_{op}, τ_0, and $\alpha\tau_{op}$ Values of the bzDNA13–Zα_{ADAR1} Complexes at P/N = 0, 0.3, and 0.9 Determined by TRIS-Catalyzed NMR Exchange Experiments at 35 °C[a]

	base pair	P/N = 0	P/N = 0.3	P/N = 0.9
αK_{op} ($\times 10^{-6}$)	T0·A0	94 ± 10	100 ± 2	105 ± 3
	G1·C1′	0.76 ± 0.03	0.95 ± 0.02	1.31 ± 0.05
	G2·C2′	1.13 ± 0.02	1.39 ± 0.02	2.03 ± 0.09
	C3·G3′	1.79 ± 0.14	2.09 ± 0.07	2.40 ± 0.16
	G4·C4′	0.90 ± 0.03	1.11 ± 0.05	1.17 ± 0.08
	C5·G5′	0.66 ± 0.03	0.73 ± 0.02	0.93 ± 0.04
	G6·C6′	4.43 ± 0.36	5.61 ± 0.22	5.89 ± 0.25
	C7·G7′	95 ± 73	105 ± 41	n.d.
τ_0 (ms)	G1·C1′	<1	29 ± 5	106 ± 7
	G2·C2′	6 ± 5	28 ± 3	61 ± 6
	C3·G3′	48 ± 12	56 ± 4	82 ± 8
	G4·C4′	61 ± 8	89 ± 9	122 ± 13
	C5·G5′	54 ± 21	80 ± 10	138 ± 8
	G6·C6′	15 ± 5	22 ± 2	27 ± 2
$\alpha\tau_{op}$ (ns)	G1·C1′	n.d.	27 ± 5	221 ± 18
	G2·C2′	6 ± 5	40 ± 5	125 ± 13
	C3·G3′	85 ± 22	116 ± 9	196 ± 23
	G4·C4′	55 ± 7	99 ± 11	142 ± 18
	C5·G5′	36 ± 14	59 ± 7	128 ± 10
	G6·C6′	68 ± 23	122 ± 12	158 ± 14

[a]n.d.: not determined.

intercept is τ_0 (see eq 3). In the bzDNA13–Zα_{ADAR1} complexes, all G·C base pairs have larger αK_{op} values (smaller slopes) and longer τ_0 (larger *y*-intercepts) than those of free bzDNA13 (Table 1 and Figure 6). For example, the G1·C1′ base pair in the bzDNA13–Zα_{ADAR1} complex at P/N = 0.9 has 2-fold larger αK_{op}, 10-fold longer τ_0, and 20-fold longer $\alpha\tau_{open}$ than that of free bzDNA13 (Table 1). Similar effects are also observed in other G·C base pairs in region I (Table 1). This demonstrates that when bzDNA13 duplex interacts with Zα_{ADAR1} in the initial contact conformation, the G·C base pairs are opened more slowly and closed much more slowly compared to free bzDNA13. At the same time, the G·C base pairs in the bzDNA13–Zα_{ADAR1} complex become slightly less stable than the corresponding base pairs in the free bzDNA13 duplex. Although the G·C base pairs in the initial contact conformation became less dynamic by interaction with Zα_{ADAR1}, the longer lifetime of their open states could provide the window needed for the B–Z transition of the CG-rich region.

DISCUSSION

Left-handed Z-DNA is a higher energy conformation and forms with help of high-salt concentration, negative supercoiling,[1,2] or binding of Z-DNA binding proteins.[5−9] The Zα domains of various Z-DNA binding proteins display similar binding modes with a 6-bp DNA, d(CGCGCG)$_2$, in which one Zα domain binds to one strand of double-stranded Z-DNA, while a second monomer binds to the opposite strand, yielding two-fold symmetry with respect to the DNA helical axis.[5,6,8] This 6-bp B-DNA duplex is converted to Z-DNA by the Zα proteins via an active B–Z transition mechanism, in which the Zα_{ADAR1} protein first binds to B-DNA and then converts it to left-handed Z-DNA, a conformation that is then stabilized by the binding of a second Zα_{ADAR1} molecule.[12,21] The Zα proteins can also bind to 6-bp non-CG repeat DNA, e.g., d(CACGTG)$_2$ and d(CGTACG)$_2$, and induce a B–Z transition through a common Z-DNA binding mode.[22] However, these structural studies were limited to short 6-bp DNA duplexes and thus cannot provide detailed information about Z-DNA production in a long genomic DNA. The X-ray structural study of the 15-bp DNA duplex, the CG-rich DNA segment spans eight base-pairs and requires four molecules of Zα_{ADAR1} protein; two molecules (A and B in Figure 7) bind to one strand of the Z-DNA segment, while the other two molecules (C and D in Figure 7) bind to the opposite strand.[13] This study also found that bases between B- and Z-DNA are continuously stacked with the breaking of only one base pair at the junction and extrusion of each base.[13] However, the existence of base extrusion of only one base pair still cannot answer the question of how Z-DNA binding protein selectively induces the B–Z transition in the CG-rich DNA segment while maintaining the B-conformation of other segments and the integrity of the overall helix.

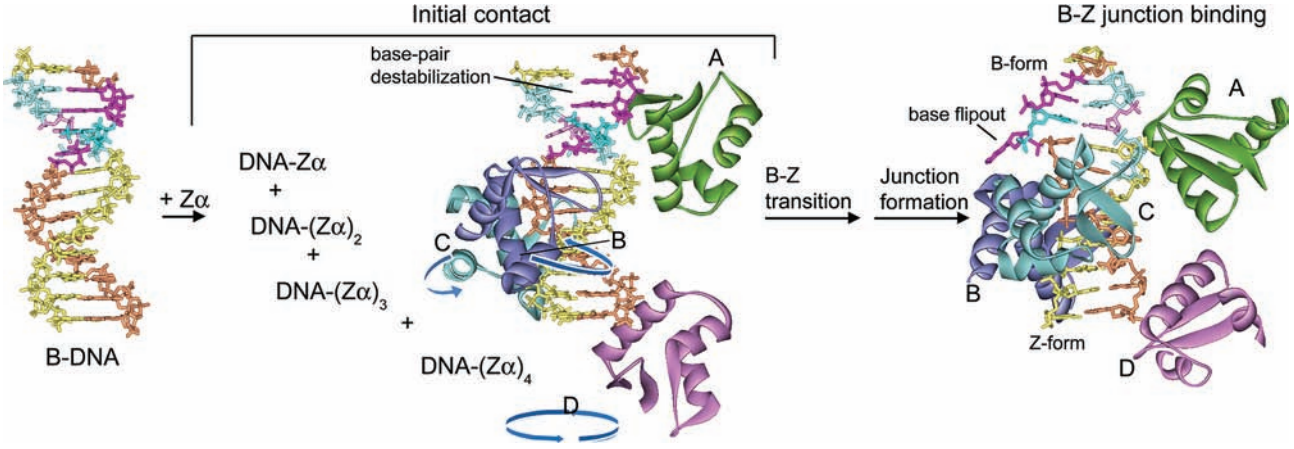

Figure 7. Suggested mechanism of B–Z junction formation in bzDNA13, induced by four molecules of Zα_{ADAR1}. Four Zα_{ADAR1} proteins are colored green (molecule A), purple (molecule B), cyan (molecule C) and pink (molecule D). In the bzDNA13, one strand is colored orange, cyan, and magenta and the other is colored yellow, light cyan, and light magenta to distinguish the two strands. Yellow and orange indicate G or C residues, magenta and light magenta indicate A residues, and cyan and light cyan indicate T residues. Blue arrows indicate relative movement of each molecule to induce the helical unwinding of a DNA duplex and to establish the B–Z junction binding conformation based on active B–Z transition mechanism suggested by our previous study.[12]

dx.doi.org/10.1021/ja211581b | J. Am. Chem. Soc. 2012, 134, 5276–5283

Our study demonstrates the initial contact conformation as an intermediate structure during B−Z junction formation induced by $Z\alpha_{ADAR1}$ (Figure 7). The unique structural features of the bzDNA13 and $Z\alpha_{ADAR1}$ in the initial contact conformation explain how the CG-rich region in a long genomic DNA can be selectively converted to Z-DNA by Z-DNA binding proteins. First, in the initial contact conformation, the $Z\alpha_{ADAR1}$ protein displays unique backbone conformational changes, but bzDNA13 maintains the B-form helix. In the $Z\alpha_{ADAR1}$−bzDNA13 complex at P/N ≤ 1, the residues of $Z\alpha_{ADAR1}$ underwent $\Delta\delta_{avg}$ < 0.15 ppm upon binding to bzDNA13, whereas the significant chemical shift changes were observed in the $\beta1-\alpha2$ and $\beta2-$loop$-\beta3$ regions of the $Z\alpha_{ADAR1}$−CG6 complex (Figure 2b). In addition, in the $Z\alpha_{ADAR1}$−bzDNA13 complex at P/N ≤ 1, the amide resonances for five residues (173−177) of the $\alpha3$ helix disappeared altogether (Figure 2b). These results meant that, in the initial contact conformation, the $Z\alpha_{ADAR1}$ binds to bzDNA13 mainly through the $\alpha3$ helix contrast to the $Z\alpha_{ADAR1}$−Z-DNA complex. Surprisingly, all ^{31}P spectra of the bzDNA13−$Z\alpha_{ADAR1}$ complex at P/N ≤ 1 showed the same chemical shift dispersion as that of free bzDNA13 (Figure 1c). This observation indicates that the bzDNA13 duplex is not yet converted to Z-DNA but maintains a B-form helix, even though the backbone conformation of $Z\alpha_{ADAR1}$ is affected by the DNA−protein interaction.

Second, in the initial contact conformation, the $Z\alpha_{ADAR1}$ protein interacts with the CG-rich region I rather than AT-rich region II of bzDNA13. This is supported by the NOESY data of free bzDNA13 and the bzDNA13−$Z\alpha_{ADAR1}$ complex (Figure 5) and a previous NMR study in which the $Z\alpha_{ADAR1}$ exhibits the sequence preference of $d(CGCGCG)_2 \gg d(CACGTG)_2 > d(CGTACG)_2$.[23] It was also reported that the $Z\alpha_{ADAR1}$ preferentially binds to free B-form of $d(CGCGCG)_2$, rather than the 1:1 DNA−$Z\alpha_{ADAR1}$ complex.[12,21] This finding strongly suggests that the major complex state of $Z\alpha_{ADAR1}$ in the initial contact conformation formed at P/N ratio ≤1 is not the $\mathbf{DP}_4$ complex (bzDNA13 denoted as **D** and $Z\alpha_{ADAR1}$ denoted as **P**) but may be a mixture of the various complex states such as **DP**, $\mathbf{DP}_2$, and $\mathbf{DP}_3$. The existence of these complexes in the complete complex population at P/N ratio ≤ 1 was confirmed by the line broadening of the resonances in the ^{31}P NMR spectra assigned to the B-form (Figure 1c).

Third, the AT-rich region II of bzDNA13 becomes significantly destabilized by formation of the initial contact conformation and then formed a bubble-like structure even though the $Z\alpha_{ADAR1}$ interacts not with the AT-rich region II but with CG-rich region I (Figure 7). The B−Z transition of DNA duplexes involves conformational change from right-handed B-DNA to left-handed Z-DNA. During this process, the ζ/α backbone torsion angles, which exhibited gauche−/gauche− in B-DNA, became gauche+/gauche+ conformation at CpG step and gauche−/trans conformation at GpC step in Z-DNA (Table S3, Supporting Information). In the bzDNA13−$Z\alpha_{ADAR1}$ complex, the CG-rich region I shows the same backbone conformation with Z-DNA, while the ζ/α torsion angles of the AT-rich region II, except B−Z junction site, exhibit gauche−/gauche− conformation like B-DNA (Table S3, Supporting Information). In order to establish the Z-DNA conformation, the $Z\alpha_{ADAR1}$ proteins should induce the movement of each strand of a DNA duplex to produce the helical unwinding as shown in Figure 7. In the case of short CG-rich DNA duplexes such as $d(CGCGCG)_2$, these helical unwindings could have occurred easily because there are no constraints in the movement of each strand of duplexes. However, the neighboring AT-rich region II can strongly interfere with the helical movement of the CG-rich region I because the AT-rich region II will remain as B-DNA. Interestingly, we first found the bubble-like structure of the bzDNA13 in the initial contact conformation, supported by the hydrogen exchange study of bzDNA13 (Figure 4). The flexible bubble-like structure of the AT-rich region II allows the CG-rich region I to convert easily to Z-DNA, like an 8-bp CG-rich DNA duplex. In the bzDNA13−$Z\alpha_{ADAR1}$ complex, the B−Z junction site shows the unusual ζ/α backbone conformation (A−1pT0 step: gauche−/gauche+, A0′pT−1′ step: cis/gauche +) (Table S3, Supporting Information).

Forth, the $Z\alpha_{ADAR1}$ protein causes that the G·C base pairs of region I to open and reclose more slowly compared to free bzDNA13 and provides more time for the B−Z transition to occur. The B−Z transition involves each base-pair flipping upside down.[1] During the B−Z transition process, the G·C base pairs are opened and then each dG and dC bases flip over into opposite direction.[1] The dC remains in the anti conformation because both the base and sugar flip over, while the inversion of only the base causes dG into the syn conformation.[1] In the bzDNA13, the B−Z transition rarely occurred in contrast to $d(CGCGCG)_2$, because the stable G·C base pairs interfere with the base-pair flipping upside down. Base-pair opening kinetics study revealed that the $Z\alpha_{ADAR1}$ in the initial contact conformation significantly increased the lifetimes for opening states of the G·C base pairs (Table 1). The longer lifetimes for opening states provide more time for the base-pair flipping to occur, and then the B-form helix of the CG-rich region I can be changed to left-handed Z-DNA. When the P/N ratio rose to ≥2, the added $Z\alpha_{ADAR1}$ preferred to bind to the various complex states, producing the $\mathbf{DP}_4$ complex, because free B-DNA rarely existed under these conditions. And then the CG-rich region I in the $\mathbf{DP}_4$ complex could be converted to Z-conformation (Figure 7). This analysis was strongly supported by the ^{1}H/^{15}N-HSQC spectrum of the $Z\alpha_{ADAR1}$−bzDNA13 complex at P/N = 2, where some amide resonances exhibited two signals; one was close to signal for the initial contact conformation, and the other to that for the $Z\alpha_{ADAR1}$−Z-DNA complex (Figure 3). After B−Z transition of the CG-rich region I, the AT-rich region II forms base pairs, and then the B−Z junction structure, in which the bases of the T0·A0′ base pair are extruded to maintain continuous base stacking between B-DNA and Z-DNA,[13] is formed.

■ SUMMARY

We investigated the kinetics and thermodynamics of base-pair openings of bzDNA13 in complex with $Z\alpha_{ADAR1}$ at various P/N ratios using TRIS as a base catalyst. The chemical shift perturbation of the amide backbone of $Z\alpha_{ADAR1}$ by bzDNA13 was also studied as a function of the P/N ratios. Our study demonstrates the initial contact conformation as an intermediate structure during B−Z junction formation induced by $Z\alpha_{ADAR1}$, in which the $Z\alpha_{ADAR1}$ protein displays unique backbone conformational changes, but bzDNA13 maintains the B-form helix. We also found the unique structural features of the bzDNA13 in the initial contact conformation: (i) instability of the AT-rich region II and (ii) longer lifetime for opening state of the CG-rich region I. Based on this study, we suggest a mechanism for B−Z junction formation in long genomic DNA: (i) the $Z\alpha_{ADAR1}$ specifically interacts with a CG-

rich DNA segment in a DNA helix via initial contact conformation; (ii) the two neighboring AT-rich regions become very unstable and form bubble-like structures and the CG-rich segment in the middle of two bubble-like structures easily converts to Z-DNA like $d(CGCGCG)_2$; and (iii) the bases of the neighboring AT-rich region are base-paired again, and the B−Z junction structure is formed.

■ ASSOCIATED CONTENT

Supporting Information

Exchange rate constants and 1D ^{1}H and ^{31}P NMR spectra of free bzDNA13 and the bzDNA13−$Z\alpha_{ADAR1}$ complex. This material is available free of charge via the Internet at http://pubs.acs.org.

■ AUTHOR INFORMATION

Corresponding Author

joonhwa@gnu.ac.kr; byongseok.choi@kaist.ac.kr

Author Contributions

#These authors contributed equally.

Notes

The authors declare no competing financial interest.

■ ACKNOWLEDGMENTS

This work was dedicated to Professor Woo Song Ha, Former President of Gyeongsang National University. This work was supported by the National Research Foundation of Korea grants (2010−0014199, NRF-C1ABA001−2010−0020480 to J.-H.L. and 2009−0092818, 2009−220-C00036, 2011-0020322 to B.-S.C.) funded by the Korean Government (MEST). This work was also supported by a grant from Next-Generation BioGreen 21 Program (SSAC, no. PJ008109), Rural Development Administration, Korea. We thank the KIST NMR Facility and GNU Central Instrument Facility for performing NMR experiments and Melissa Stauffer, of Scientific Editing Solutions, for editing the manuscript.

■ REFERENCES

(1) Herbert, A.; Rich, A. *J. Biol. Chem.* **1996**, *271*, 11595.
(2) Herbert, A.; Rich, A. *Genetica* **1999**, *106*, 37.
(3) Pohl, F. M.; Jovin, T. M. *J. Mol. Biol.* **1972**, *67*, 375.
(4) Wang, A. H.; Quigley, G. J.; Kolpak, F. J.; Crawford, J. L.; van Boom, J. H.; van der Marel, G.; Rich, A. *Nature* **1979**, *282*, 680.
(5) Schwartz, T.; Rould, M. A.; Lowenhaupt, K.; Herbert, A.; Rich, A. *Science* **1999**, *284*, 1841.
(6) Schwartz, T.; Behlke, J.; Lowenhaupt, K.; Heinemann, U.; Rich, A. *Nat. Struct. Biol.* **2001**, *8*, 761.
(7) Kim, Y.-G.; Muralinath, M.; Brandt, T.; Pearcy, M.; Hauns, K.; Lowenhaupt, K.; Jacobs, B. L.; Rich, A. *Proc. Natl. Acad. Sci. U.S.A.* **2003**, *100*, 6974.
(8) Ha, S. C.; Lokanath, N. K.; Van Quyen, D.; Wu, C. A.; Lowenhaupt, K.; Rich, A.; Kim, Y. G.; Kim, K. K. *Proc. Natl. Acad. Sci. U.S.A.* **2004**, *101*, 14367.
(9) Ha, S. C.; Kim, D.; Hwang, H. Y.; Rich, A.; Kim, Y. G.; Kim, K. K. *Proc. Natl. Acad. Sci. U.S.A.* **2008**, *105*, 20671.
(10) Schade, M.; Turner, C. J.; Kuhne, R.; Schmieder, P.; Lowenhaupt, K.; Herbert, A.; Rich, A.; Oschkinat, H. *Proc. Natl. Acad. Sci. U.S.A.* **1999**, *96*, 12465.
(11) Rothenburg, S.; Deigendesch, N.; Dittmar, K.; Koch-Nolte, F.; Haag, F.; Lowenhaupt, K.; Rich, A. *Proc. Natl. Acad. Sci. U.S.A.* **2005**, *102*, 1602.
(12) Kang, Y.-M.; Bang, J.; Lee, E.-H.; Ahn, H.-C.; Seo, Y.-J.; Kim, K. K.; Kim, Y.-G.; Choi, B.-S.; Lee, J.-H. *J. Am. Chem. Soc.* **2009**, *131*, 11485.
(13) Ha, S. C.; Lowenhaupt, K.; Rich, A.; Kim, Y. G.; Kim, K. K. *Nature* **2005**, *437*, 1183.
(14) Delaglio, F.; Grzesiek, S.; Vuister, G. W.; Zhu, G.; Pfeifer, J.; Bax, A. *J. Biomol. NMR* **1995**, *6*, 277.
(15) Goddard, T. D.; Kneller, D. G. *SPARKY 3*; University of California: San Francisco, CA, 2003.
(16) Lee, J.-H.; Pardi, A. *Nucleic Acids Res.* **2007**, *35*, 2965.
(17) Lee, J.-H.; Jucker, F.; Pardi, A. *FEBS Lett.* **2008**, *582*, 1835.
(18) Bang, J.; Bae, S.-H.; Park, C.-J.; Lee, J.-H.; Choi, B.-S. *J. Am. Chem. Soc.* **2008**, *130*, 17688.
(19) Bang, J.; Kang, Y.-M.; Park, C.-J.; Lee, J.-H.; Choi, B.-S. *FEBS Lett.* **2009**, *583*, 2037.
(20) Gueron, M.; Leroy, J. L. *Methods Enzymol.* **1995**, *261*, 383.
(21) Lee, E.-H.; Seo, Y.-J.; Ahn, H.-C.; Kang, Y.-M.; Kim, H.-E.; Lee, Y.-M.; Choi, B.-S.; Lee, J.-H. *FEBS Lett.* **2010**, *584*, 4453.
(22) Ha, S. C.; Choi, J.; Hwang, H. Y.; Rich, A.; Kim, Y. G.; Kim, K. K. *Nucleic Acids Res.* **2009**, *37*, 629.
(23) Seo, Y.-J.; Ahn, H.-C.; Lee, E.-H.; Bang, J.; Kang, Y.-M.; Kim, H.-E.; Lee, Y.-M.; Kim, K.; Choi, B.-S.; Lee, J.-H. *FEBS Lett.* **2010**, *584*, 4344.